

Convective and Stratiform Cloud Rainfall Estimation from Geostationary Satellite Data

Li Jun (李俊), Wang Luyi (王路易) and Zhou Fengxian (周凤仙)

Institute of Atmospheric Physics, Chinese Academy of Sciences, Beijing 100029

Received December 17, 1992; revised March 12, 1993

ABSTRACT

The Bayes Decision (BD) method was used to distinguish the convective and stratiform components of cloud systems from GMS-4 satellite data. A technique originally developed by Adler and Negri (1988, hereafter abbreviated AN) was improved for estimating the convective and stratiform cloud precipitation areas and rates of cloud systems from GMS satellite imagery. It has been applied to a tropical cyclonic cloud cluster observed over east coast area of China on September 23, 1992, which brought about flood disaster in that region. Overlaid 6-hour surface rainfall observations show that the rainfall areas and amounts match with results from improved AN technique. The successful application of the Adler and Negri's technique to convective and stratiform clouds provides encouragement for the use of this method over large region of mid-latitude China where radar data are not fully covered.

Key words: Rainfall estimation, Classification, Rainfall rate and area

1. INTRODUCTION

The heavy precipitation in mid-latitude China is caused by cloud systems associated with tropical cyclone, local deep convection, stationary front, frontal cyclone etc. The convective cloud system usually produces heavy rain with short duration while the precipitation caused by stratiform clouds can last a few hours to several days with large amount of accumulated rainfall. Since the physical and dynamical processes of air motion in the convective and stratiform clouds are different, the important thing is to distinguish the two components from the cloud systems. In 1988, Adler and Negri proposed a technique by using the geosynchronous IR data to separate the convective and stratiform parts from the mesoscale cloud systems. They tested their algorithm, referred to as the Convective-Stratiform Technique (CST), on data from the Geosynchronous Operational Environmental Satellite (GOES) IR (10.5–12.6 μm) channel obtained during four days of the second Florida Area Cumulus Experiment (FACE). Also, Goldenberg, Houze and Churchill (1990, abbreviated GHC) applied the modified CST to the analysis of a cloud cluster observed in the Winter Monsoon Experiment (WMONEX) over the South China Sea. Results both from FACE and WMONEX agreed with data from surface observation and aircraft measurement.

One main effort of CST is to distinguish the convective and stratiform components from mesoscale cloud systems. The difficulty in identifying them is that the technique is not readily transferable from location to location. To avoid this inadequacy, we use the Bayes Decision method to identify the convective and stratiform clouds automatically from satellite images. The initial classification criteria are created from the dynamical clustering technique over training area using both visible and infrared information of satellite images. The different

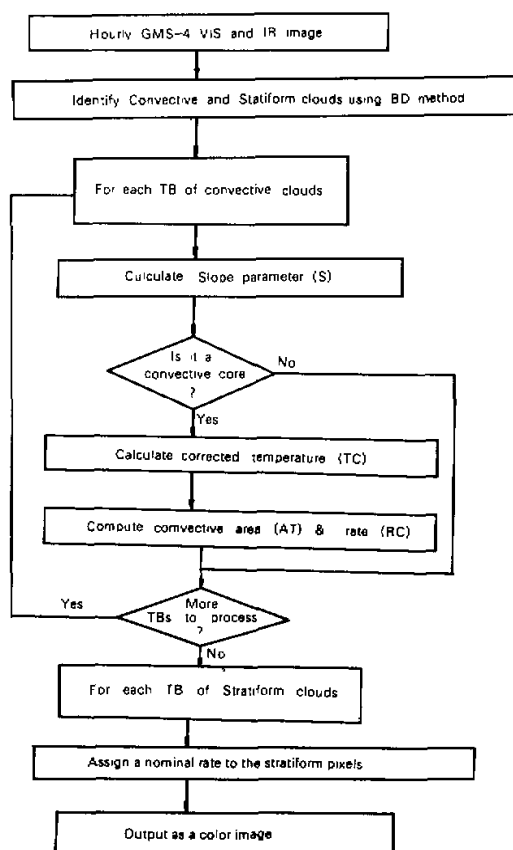


Fig.1. Flow chart of improved CST technique.

cloud system adopts the different criterion which is adapted after each BD classification process to gain the classification accuracy. Then the rain rate and area are calculated based on the IR brightness temperature (T_B) and cloud model approach. The use of one-dimensional cloud model to account for ambient temperature, moisture and shear conditions provides a stronger physical (less empirical) basis for the cloud-height / rain relationships. It potentially allows for the transportability of the technique to various climatological regimes.

II. IMPROVED CST

1. Flow Chart

According to the procedure of rainfall estimation described above, we draw a flow chart (Fig.1) and call it as improved CST technique.

The final product is a color image with different colors denoting different rain rates.

2. Bayes Decision Method

The purpose of classification is to sort GMS-4 visible and infrared image data into several classes including convective and stratiform clouds. The Bayes Decision rule is a criterion

for partitioning a feature vector X to class W_i from classes ($i=1,2,\dots,m$), and states that: $X \in W_i$, if and only if

$$P(X|W_i)P(W_i) \geq P(X|W_j)P(W_j) \quad (1)$$

for all $j=1,2,\dots,m$. Where $P(X|W_i)$ is the conditional probability that the feature vector has value X and is in class W_i , and $P(W_i)$ is the prior probability of class W_i given image. The detailed procedure is described in another paper (Li et al., 1992).

3. Location of Convective Cores on the Infrared Image

After the convective area is identified by BD, a "slope parameter" (S) is calculated for each TB of convective area to measure the strength of the TB as described in GHC

$$S = \frac{\bar{\Delta}}{4} \left[\frac{T_{i-2,j} + T_{i+2,j} + 2(T_{i-1,j} + T_{i+1,j}) - 6T_{i,j}}{4\Delta_{EW}} + \frac{T_{i,j-1} + T_{i,j+1} - 2T_{i,j}}{\Delta_{NS}} \right], \quad (2)$$

where i, j refer to the position of the pixel for which S is calculated; Δ_{EW} and Δ_{NS} are the GMS-4 east-west and north-south resolutions respectively; and $\bar{\Delta}$ is the average GOES distance (from AN) to the six surrounding pixels. Twice as many pixels are used for the calculation in the east-west (i) as in the north-south (j) direction to be consistent with the difference in resolution.

The (TB, S) pairs are then compared to an empirical "discrimination line" to distinguish which TBs are associated with convective cores. According to GHC a minimum value is set to indicate the location of a convective core if

$$S \geq \exp[0.0826(TB - 207)] \quad (3)$$

We found this result could also be applied to mid-latitude region of China.

4. Estimation of Area Covered by Convective Precipitation

The next step in the modified CST is to assign a real coverage of precipitation [AC_i (km^2)] to each of the cores selected through the screening process described in Section 3.2. The index i refers to the i -th core. To assign the rainfall area, we follow GHC in assuming that $\ln(AC_i)$ is directly proportional to cell-top height, which is indicated by cloud-top temperature as follows:

$$\ln(AC_i) = aTC_i + b, \quad (4)$$

where $a = -0.0465$ and $b = 15.27$ are constants, and TB , as in GCH, is replaced by the variable TC_i , which is the cloud-top temperature of the i -th convective core corrected for the difference in resolution between the satellite data and the one-dimensional cloud model of Adler and Mack (1984).

5. Rain Rate in the Convective Area

To obtain an estimate of the average rain rate RC_i ($\text{kg} \cdot \text{m}^{-2} / \text{h}$) in the area AC_i associated with the i -th core, we continue to follow GHC by using the model of Adler and Mack (1984) to calculate the time rate for the fallout of condensed water mass VR_i ($\text{kg} \cdot \text{m}^{-2} / \text{h}$) as a function of TC_i , and then the rainfall rate as a function of TC_i is as follows:

$$\ln(RC_i) = eTC_i + f, \quad (5)$$

where $e = -0.0157$ and $f = 4.76$. In our study, e and f are -0.0257 and 7.068 respectively in order to fit the application over East China.

6. Assignment of Stratiform Cloud Rain Rate

The next step in applying CST is to assign rain rate to the stratiform cloud regions. The method used by AN was to assign a nominal rain rate of $2 \text{ kg} \cdot \text{m}^{-2} / \text{h}$ (i.e., $2 \text{ mm} / \text{h}$) to the pixels classified by BD method as stratiform cloud in a very thorough and careful analysis of rain rates in GATE cloud clusters. Leary (1984) also found $2 \text{ kg} \cdot \text{m}^{-2} / \text{h}$ to be the typical rain rate in the stratiform cloud regions. Also, the overall (area-weighted) mean stratiform cloud rain rate obtained by GHC is almost exactly $2 \text{ kg} \cdot \text{m}^{-2} / \text{h}$. In view of these observations, it seems reasonable to adopt the average rate of $2 \text{ kg} \cdot \text{m}^{-2} / \text{h}$ assumed by AN in this study. Results also show that 1 and $3 \text{ kg} \cdot \text{m}^{-2} / \text{h}$ are probably the reasonable lower and upper limits for the stratiform rate.

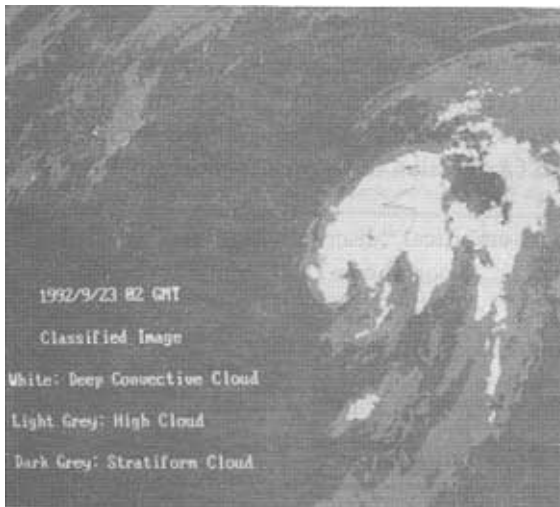


Fig.2. 7 class cloud image of 02 GMT, Sept. 23, 1992. (original: color)



Fig.3. IR facsimile cloud image of 02 GMT, Sept. 23, 1992.



Fig.4. Rainfall area and rate estimation from satellite classified image. (original: color)



Fig.5. Overlaid 6-hour Rainfall Obs.(mm) on the Classified Image.

III. APPLICATION OF IMPROVED CST IN EAST CHINA

The satellite data set used in this study is obtained from the Hydrological Forecasting & Water Control Center, Ministry of Water Resources. We have used only the hourly GMS-4 IR and VIS data from 01 to 06 GMT on Sept. 23, 1992. It is a case of landed Typhoon No.13 over South-east coast area of China. The 6-hour (01-06 GMT) rainfall observations were used for comparison. The region of application is from 95° to 135° east longitude and 20° to 40° north latitude. First, the Bayes Decision method was used to classify the hourly satellite data into a 7-class cloud image which includes convective and stratiform components. Fig.2 shows 7 class cloud image from IR and VIS images of 02 GMT, while Fig.3 is an IR facsimile cloud image of the same time for comparison. The convective and stratiform components in Fig.2 are well corresponding to the convective and stratiform clouds in Fig.3. Fig.4 is rainfall area and rate image of the same time based on the algorithm described in Fig.1 with colors which denote the rain rate ranges. The convective areas cover parts of Zhejiang, Jiangxi and

Table 1. Comparison of Satellite Estimation with 6-hour Rainfall Observations more than 19 mm/h

Location		Satellite Estimation (mm/h)						Sum	Obs.	Rel.Err.(%)
Lat.	Long.	01	02	03	04	05	06	Sum	01-06	(Sum-Obs.)/Obs.
31.32	120.63	0.0	6.1	7.4	7.4	6.7	5.0	32.6	28	+16.4
31.07	120.43	6.4	7.1	7.4	7.4	5.8	3.7	37.8	36	+ 5.0
30.97	120.12	4.2	6.1	8.1	7.4	6.1	5.5	37.4	42	-11.0
28.97	118.87	7.1	7.4	6.7	4.7	2.0	2.0	29.9	46	-35.0
35.22	106.68	2.0	2.0	2.0	2.0	2.0	3.7	13.7	20	-31.5
31.20	120.65	6.1	6.1	7.4	6.7	6.1	5.0	37.4	34	+10.0
30.23	120.17	6.7	7.2	7.4	5.5	5.8	4.7	37.3	49	-23.9
30.87	120.10	5.2	6.7	7.4	6.7	5.5	5.5	37.0	52	-28.8
30.63	121.10	7.1	6.7	6.1	7.1	5.0	4.7	36.7	56	-34.5
30.35	119.42	4.7	6.7	6.1	6.7	6.1	5.0	35.3	23	+53.5
29.43	120.98	8.1	8.1	6.4	5.8	6.1	5.8	40.3	27	+49.3
34.50	106.70	2.0	2.0	2.0	2.0	2.0	2.0	12.0	22	-45.5
35.03	106.52	2.0	2.0	2.0	2.0	2.0	2.0	12.0	23	-47.8
31.45	120.43	2.0	0.0	6.8	5.8	6.4	4.7	25.7	21	+22.4
31.00	120.63	6.4	6.1	7.7	6.7	0.0	3.7	30.6	52	-41.2
29.87	121.57	8.1	9.1	6.7	5.8	4.7	4.2	38.6	29	+33.1
29.70	120.23	6.7	6.4	5.5	3.9	2.0	2.0	26.5	40	-33.8
29.60	120.82	8.4	6.7	6.1	5.5	5.0	5.8	37.5	28	+33.9
29.12	119.65	7.1	5.5	4.2	3.9	2.0	2.0	24.7	22	+12.3
27.92	118.53	5.2	4.4	0.0	0.0	3.9	2.0	15.5	20	-22.5
30.73	122.45	6.1	6.1	6.1	7.4	6.7	6.1	38.5	44	-12.5
30.03	122.12	7.4	7.4	7.7	5.8	5.5	2.0	35.4	45	-21.3
28.82	120.92	7.1	0.0	4.7	6.1	4.2	4.4	26.5	25	+ 6.0
28.08	119.13	5.2	4.4	2.0	2.0	2.0	2.0	17.6	40	-56.0
28.08	121.28	6.1	4.4	3.7	4.2	2.0	0.0	20.4	21	- 2.9
34.90	105.67	2.0	2.0	2.0	4.2	2.0	2.0	14.2	20	-29.0
34.38	107.05	2.0	2.0	2.0	2.0	2.0	2.0	12.0	24	-50.0
32.07	121.60	2.0	0.0	5.8	5.8	6.1	6.1	23.8	22	+ 8.2
30.27	119.83	5.5	7.7	7.1	5.8	4.7	3.9	34.7	68	-49.0
30.77	120.75	6.7	7.4	6.4	6.7	0.0	2.0	29.2	57	-48.8
30.13	118.17	0.0	6.4	0.0	0.0	2.0	6.4	14.8	22	-32.7
28.98	118.87	8.4	8.4	6.4	4.7	2.0	2.0	31.9	46	-30.7

Fujian provinces. Fig.5 shows overlaid 6-hour cloud rainfall observations on Fig.2. One can see that the rainfall areas determined from satellite data match with ground truth (Fig.4) quite well. Table 1 lists the comparison of satellite estimation with surface observations.

Table 1 shows that the locations with more than 19 mm / h rainfall observation within 6 hours mainly corresponding to the convective cloud areas in satellite data. If we consider the rainfall estimation is true when the relative error $Err = (\text{sum} - \text{obs.}) / \text{obs.}$ is less than 35%, then the true rate of convective rainfall estimation is about 72% according to Table 1. Also, the rainfall estimation method was used in the real-time GMS-4 data processing system at Hydrological Forecasting & Water Control Center, Ministry of Water Resources. Experiments and applications show that this technique plays an important role in heavy rain monitoring during the precipitation seasons in 1991 and 1992. Improvement is necessary especially in rainfall estimation for stratiform cloud.

IV. CONCLUSION

The combination of Bayes Decision method and CST technique was applied to rainfall estimation over East China. The results show that the rainfall areas estimated from GMS-4 visible and infrared data match with 6-hour surface observations. The true rate of rainfall rate estimation is about 72%. The successful application of the improved CST technique in East China encourages us to extend this method to various region of mid-latitude China. More experiments will be carried out by use of better observation data such as one-hour surface rainfall amount and radar observations in order to increase the accuracy of estimations.

The authors wish to thank Hydrological Forecasting and Water Control Center for providing the GMS-4 satellite cloud images and rainfall observation data for this study.

REFERENCES

- Adler, R. F. and A. J. Negri (1988), A satellite infrared technique to estimate tropical convective and stratiform rainfall, *J. Applied Meteorology*, **27**: 31-51.
- Adler, R. F. and R. A. Mack (1984), Thunderstorm cloud height-rainfall rate relations for use with satellite rainfall estimation techniques, *J. Clim. Appl. Meteor.*, **23**: 280-296.
- Adler, R. F., M. J. Markus and D. D. Fenn (1985), Detection of severe mid-west thunderstorms using geosynchronous satellite data, *Mon. Wea. Rev.*, **113**: 769-781.
- Goldenberg, S. B., R. A. Houze and D. D. Churchill (1990), Convective and stratiform components of a winter monsoon cloud cluster determined from geosynchronous infrared satellite data, *J. Meteor. Soc., Japan*, **68**: 37-63.
- Houze, Jr., R. A. Hobbs and P. V. Hobbs (1982), Organization and Structure of precipitating cloud systems, *Advances in Geophysics*, **41**: 3405-3411.
- Leary, C. A. (1984), Precipitation structure of the cloud clusters in a tropical easterly wave, *Mon. Wea. Rev.*, **112**: 313-325.
- Li, J. and F. X. Zhou (1990), Computer identification of multispectral satellite cloud imagery, *Advances in Atmospheric Sci.*, **7**: 366-375.
- Li, J., F. X. Zhou and L. Y. Wang (1992), Automatic classification and compression of GMS cloud imagery in heavy rainfall monitoring application, *Advances in Atmospheric Sci.*, **9**: 458-464.
- Maddox, R. A. (1980), An objective technique for separating macroscale and mesoscale features in meteorological data, *Mon. Wea. Rev.*, **108**: 1108-1121.